

See discussions, stats, and author profiles for this publication at: <https://www.researchgate.net/publication/235767937>

Janus Nanosheets of Polymer-Inorganic Layered Composites

ARTICLE *in* MACROMOLECULES · JANUARY 2012

Impact Factor: 5.8 · DOI: 10.1021/ma2021908

CITATIONS

28

READS

111

8 AUTHORS, INCLUDING:



[Ying Chen](#)

Chinese Academy of Sciences

7 PUBLICATIONS 96 CITATIONS

[SEE PROFILE](#)



[Fuxin Liang](#)

Chinese Academy of Sciences

45 PUBLICATIONS 492 CITATIONS

[SEE PROFILE](#)



[Jiaoli Li](#)

Chinese Academy of Sciences

37 PUBLICATIONS 1,349 CITATIONS

[SEE PROFILE](#)



[Dong Qiu](#)

Chinese Academy of Sciences

73 PUBLICATIONS 803 CITATIONS

[SEE PROFILE](#)

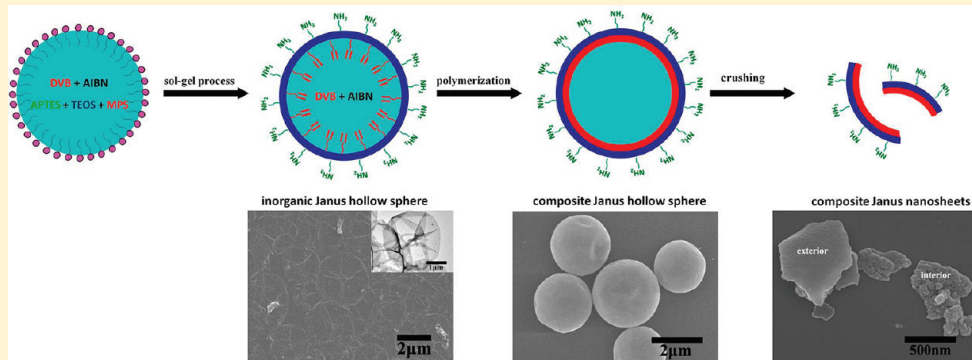
Janus Nanosheets of Polymer–Inorganic Layered Composites

Ying Chen,^{†,‡} Fuxin Liang,^{*,†} Haili Yang,[†] Chengliang Zhang,[†] Qian Wang,[†] Xiaozhong Qu,[†] Jiaoli Li,[†] Yuanli Cai,^{*,‡} Dong Qiu,[†] and Zhenzhong Yang^{*,†}

[†]State Key Laboratory of Polymer Physics and Chemistry, Institute of Chemistry, Chinese Academy of Sciences, Beijing 100190, China

[‡]College of Chemistry, Xiangtan University, Xiangtan, Hunan 411105, China

Supporting Information



ABSTRACT: Janus nanosheets of polymer–inorganic layered composites are fabricated by crushing the corresponding Janus composite hollow spheres, which are synthesized by materialization of an amphiphilic emulsion interface with self-organized sol-gel process and subsequent polymer grafting onto the lipophilic side. The Janus composite nanosheets serve as solid surfactants to stabilize emulsion droplets, which are tolerant against solvents. Janus balance of the composite nanosheets is tunable crossing from more lipophilic to hydrophilic by alteration of polymer content. Thereafter, continuous phase of the emulsions can be inverted.

1. INTRODUCTION

Janus particles with two different compositions compartmentalized distinctly onto the same surface¹ have gained increasing interests in both academic and industrial fields due to their diversity of promising performances.² For example, as solid surfactants Janus particles can easily emulsify immiscible liquids.^{3,4} Besides chemical compartmentalization, anisotropic shape of the particles can endow additional dynamic gain to make emulsions more stable due to their restricted rotation at interface.⁵ The currently reported morphologies mainly focus on two forms of particulate and rod.^{2a–c} Recently, anisotropic organic Janus nanosized discs have been synthesized by cross-linking those supramolecular structures from block copolymers.⁶ However, the polymer discs are usually swollen thus deformed in solvents. Inorganic Janus nanosheets are fabricated by multiple lithography etching onto silicon⁷ or crushing modified glass hollow spheres.⁸ They are tolerant to organic solvents. However, large-scale fabrication of Janus nanosheets remains challenging. We have recently developed a simple approach to large scale fabricate inorganic Janus nanosheets by crushing Janus hollow spheres with a nanosized shell. The Janus nanosheets act as solid emulsifiers, dry droplets of liquids form in air when continuous phase elutes due to their highly anisotropic shape.⁹ In analogy to hydrophilic–lipophilic

balance (HLB) of small surfactant molecules, the term of “Janus balance” is used to describe the hydrophilic–lipophilic balance of anisotropic particles. Janus balance of particles is usually determined by relative ratio of the two parts with varied chemistry. It is important to determine type and stability of emulsions when they serve as solid emulsifiers and to form new complex structures when as building blocks. Similar to Janus particles, it remains challenging to tune Janus balance of the nanosheets.¹⁰ We ask if the Janus balance can be further tuned from more hydrophilic to more lipophilic.

Herein, we extend our previous synthesis of inorganic Janus nanosheets to fabricate Janus nanosheets of polymer–inorganic layered composites as illustrated in Scheme 1. First, an oil in water (O/W) emulsion forms in the presence of hydrolyzed styrene–maleic anhydride copolymer (HSMA) as a surfactant.¹¹ The oil internal phase is composed of *n*-decane, oil soluble monomers for example divinylbenzene (DVB), initiator azodiisobutyronitrile (AIBN), and three silanes: tetraethyl orthosilicate (TEOS), 3-methacryloxypropyltrimethoxysilane (MPS), and γ -aminopropyltriethoxysilane (APTES).

Received: October 5, 2011

Revised: December 30, 2011

Published: January 19, 2012

Scheme 1. Schematic Synthesis of Janus Nanosheets of Polymer–Inorganic Layered Composites

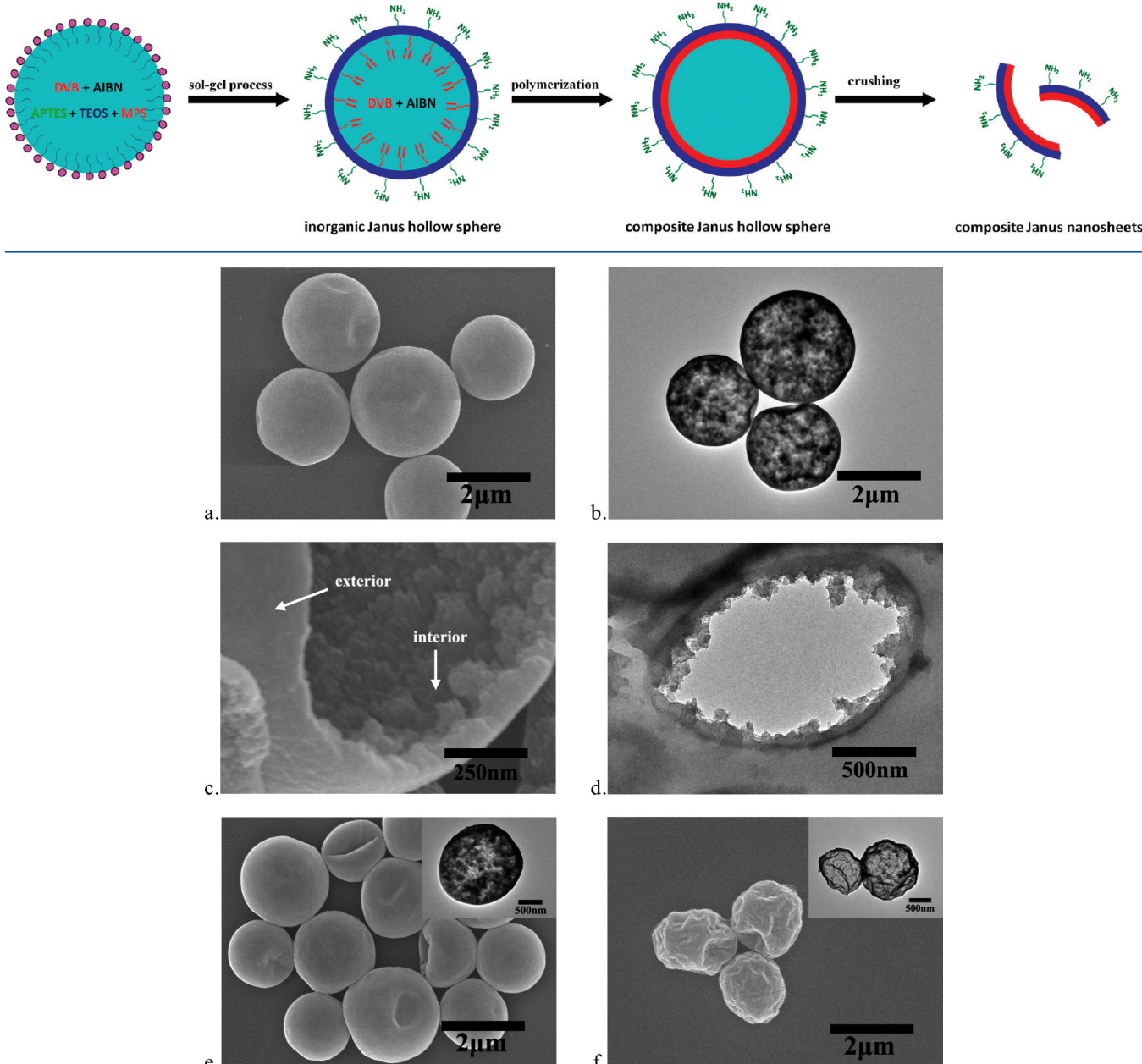


Figure 1. (a) SEM and (b) TEM images of the Janus hollow spheres with polymer–inorganic layered composite shell; (c) SEM image of a broken Janus hollow composite sphere; (d) cross-section TEM image of the Janus hollow composite sphere; (e, f) polymer and silica hollow spheres derived from the Janus hollow composite sphere after removal of silica with 10 wt % HF aqueous solution and removal of polymer by calcination at 450 °C in air, respectively.

The emulsion is kept at 25 °C for 7 h for self-organized interfacial sol–gel process under stirring. Under acidic condition, for example at pH 2.5, the sol–gel process occurs predominantly at the interface forming a smooth silica layer.¹² Onto both exterior and interior surfaces of the inorganic layer, amine- and butyl methacrylate (BMC)- groups direct external aqueous and internal oil phases, respectively. Thus, silica Janus layer forms first. Afterward, the emulsion is heated to 70 °C to initiate the polymerization of DVB onto the interior surface of the layer. While polymerization induces phase separation in the oil phase, aggregates of polydivinylbenzene (PDVB) are further grafted onto a BMC group terminated interior surface, forming a polymer layer. After dissolution of the

internal oil phase, the Janus hollow composite spheres form. By crushing the hollow spheres with colloid milling creates Janus composite nanosheets.

2. EXPERIMENTAL METHODS

2.1. Materials. 3-Methacryloxypropyltrimethoxysilane (MPS, 97%) and γ-aminopropyltriethoxysilane (APTES, 98%) were purchased from Alfa Aesar. Styrene (St, AR), azodiisobutyronitrile (AIBN, CP), *n*-decane (AR), tetraethyl orthosilicate (TEOS, AR) were purchased from Sinopharm Chemical Reagent Beijing Co. Divinylbenzene (DVB, 80%) was purchased from Sigma-Aldrich. Hydrolyzed styrene–maleic anhydride (HSMA) copolymer was synthesized by free radical polymerization.¹¹ Au nanoparticles with an average diameter of 15 nm were prepared according to Frens method.¹³ St and DVB were purified

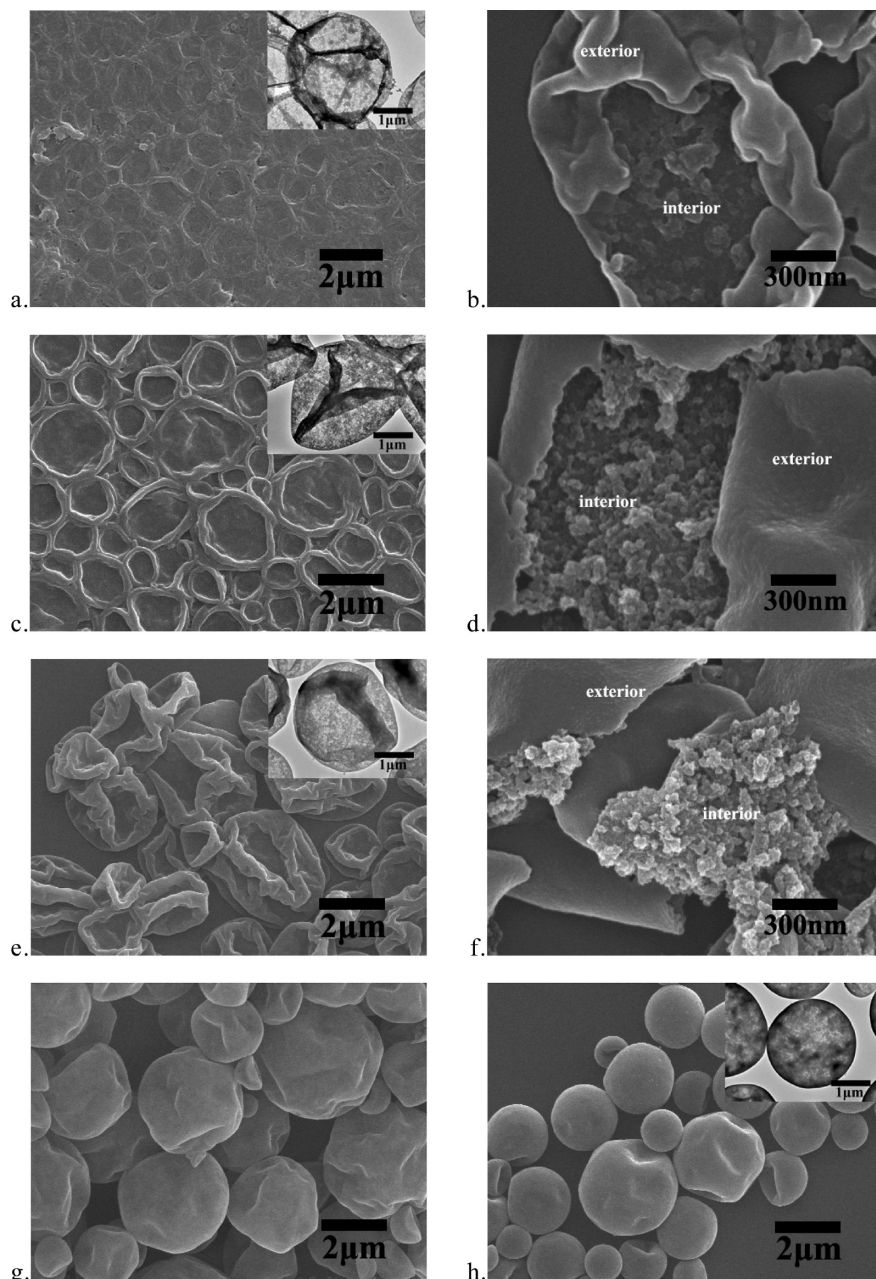


Figure 2. Morphological evolution of the Janus hollow spheres with prolonged polymerization time (h): (a, b) 0.5; (c, d) 2; (e, f) 3; (g) 8; (h) 12.

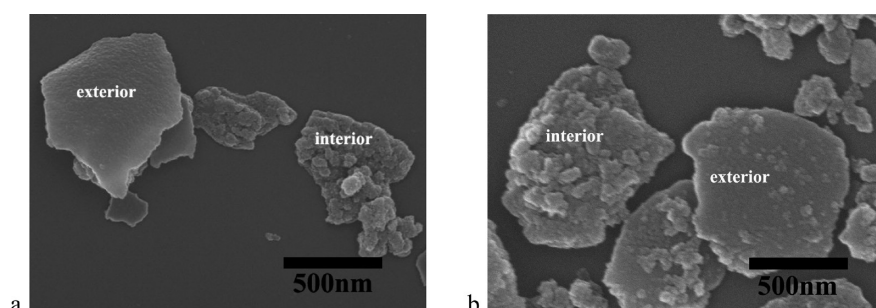


Figure 3. (a) SEM image of the Janus composite nanosheets; (b) Janus composite nanosheets after being selectively labeled with the trisodium citrate capped Au nanoparticles (about 15 nm in diameter) onto the amine-terminated side.

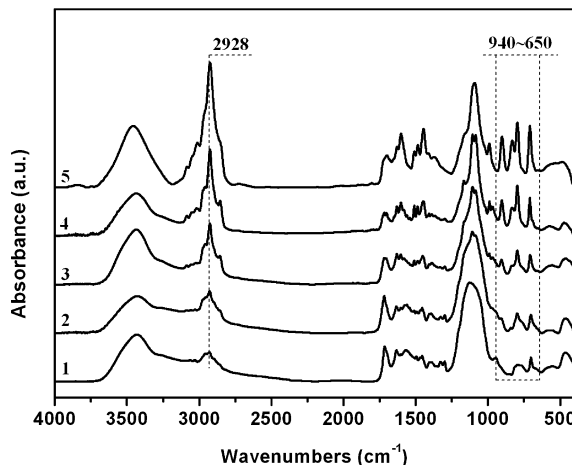


Figure 4. FT-IR spectra of some representative Janus nanosheets obtained with varied amount of DVB (g): (1) 0; (2) 5; (3) 8; (4) 10; (5) 20. Silane content is fixed at 5.2 g. The absorption peak 2928 cm^{-1} is attributed to the stretching vibration of CH_2 , the multiple absorption peaks around $940\text{--}650\text{ cm}^{-1}$ are attributed to the C-H out-of-plane bending vibration.

over Al_2O_3 column and then stored at low temperature prior to use. All other reagents were used as received without further purification.

2.2. Synthesis of the Janus Hollow Composite Spheres and the Corresponding Janus Nanosheets. An example recipe is given as follow. A 15 mL sample of 10 wt % HSMA copolymer aqueous solution was dissolved in 75 mL of water. The pH of the mixture was adjusted to 2.5 with 2 M aqueous hydrochloric acid. Then 10 g of *n*-decane, 1.1 g of APTES, 1.24 g of MPS, 5.2 g of TEOS, 10 g of DVB and 0.1 g of AIBN were mixed. The oil mixture was dispersed into the aqueous solution with a homogenizer at a speed of 12000 rpm for 5 min forming an oil-in-water emulsion. The emulsion was held under stirring at $25\text{ }^\circ\text{C}$ for 7 h for the self-organized interfacial sol-gel process of silanes. Afterward, the emulsion was heated to $70\text{ }^\circ\text{C}$ to initiate the polymerization of DVB onto the interior surface of the silica layer for 12 h. Janus hollow spheres with polymer-inorganic layered composite shell were obtained. The Janus hollow spheres were crushed into Janus nanosheets by colloid milling.

2.3. Emulsification Using the Janus Nanosheets. A given amount of the Janus nanosheets was added in a glass bottle containing 4 mL of water and 2 mL of toluene. A trace of methyl orange was introduced into water for easily distinguishing water phase. After the mixture was vigorously shaken, a water-in-oil emulsion formed. At $70\text{ }^\circ\text{C}$, a given amount of Janus nanosheets was added in a glass bottle containing 4.5 g of water and 0.5 g of paraffin (T_m : $52\text{--}54\text{ }^\circ\text{C}$). After vigorously shaken, an oil-in-water emulsion formed. When the system was cooled to room temperature, the paraffin droplets were solidified. Determination of continuous phase is according to conductivity measurement.

2.4. Characterization. Morphology of the samples was characterized using transmission electron microscopy (JEOL 100CX operating at 100 kV) and scanning electron microscopy (S-4800 at 15 kV) equipped with an energy dispersive X-ray (EDX) analyzer. The samples for SEM observation were prepared by vacuum sputtering with Pt after being ambient dried. The samples for TEM observation were prepared by spreading very dilute dispersions in ethanol onto carbon-coated copper grids and dried at room temperature. FT-IR spectroscopy was performed after scanning samples for 32 times using a Bruker EQUINOX 55 spectrometer (resolution: 4 cm^{-1}) with the sample/KBr pressed pellets. Thermogravimetric analysis (TGA) was performed using the Perkin-Elmer Pyris 1 TGA under air at a heating rate of $10\text{ }^\circ\text{C}/\text{min}$. Particle size and distribution of the sample dispersions in ethanol were measured using a Zetasizer (Nano Series, Malvern Instruments). The morphology of emulsions stabilized with the Janus nanosheets was characterized using Leica DMLP microscope.

3. RESULTS AND DISCUSSION

Under acidic condition at room temperature, self-organized interfacial sol-gel process of the three silanes occurs first, forming micrometer-sized core-shell structure with the oil phase encapsulated with the silica shell. After dissolution of the internal oil phase, hollow spheres form. Both interior and exterior surfaces of the shell are smooth (Figure S1, Supporting Information). Further labeling with acidic group capped nanoparticles reveals that the silica shell is Janus with the amine group exclusively distributed onto the exterior surface. This indicates that introduction of the initiator and monomer has no influence on formation of the Janus shell at room temperature. After formation of the Janus silica shell, the emulsion was held at $70\text{ }^\circ\text{C}$ for a free radical polymerization onto the interior surface for 12 h. Dynamic light scattering (DLS) measurement gives a mean diameter of the Janus spheres about $2\text{ }\mu\text{m}$ (Figure S2, Supporting Information). Although the exterior surface keeps smooth (Figure 1a), the interior surface becomes coarse (Figure 1b). Observation of a broken hollow composite sphere can further confirm that the interior surface is coarse and the exterior surface is smooth (Figure 1c). Cross-section TEM image of the hollow spheres clearly demonstrates that the double-layered shell is consisted of exterior dark smooth silica and interior coarse gray polymer (Figure 1d). The hollow spheres are dispersible in water but not in toluene. This means that the exterior shell surface is hydrophilic. When the hollow spheres were added into a toluene in water dispersion, toluene can be preferentially absorbed inside the cavity. This implies that the interior shell surface is lipophilic. Therefore, the hollow spheres are Janus. The corresponding PDVB hollow spheres (Figure 1e) were derived after silica was etched with dilute aqueous HF. The absence of the element Si in the EDX spectrum indicates the removal of silica in PDVB hollow spheres (Figure S3, Supporting Information). The exterior surface of the PDVB hollow spheres is smooth, indicating that there is no diffusion layer between polymer and silica. This confirms that the two steps forming silica shell and polymerization onto the interior surface are separated. Similarly, after removal of polymer by calcination at $450\text{ }^\circ\text{C}$ in air, silica hollow spheres were derived. The characteristic peaks of polymers disappear, and only the characteristic peaks assigned to silica in FT-IR spectra remain (Figure S4, Supporting Information).

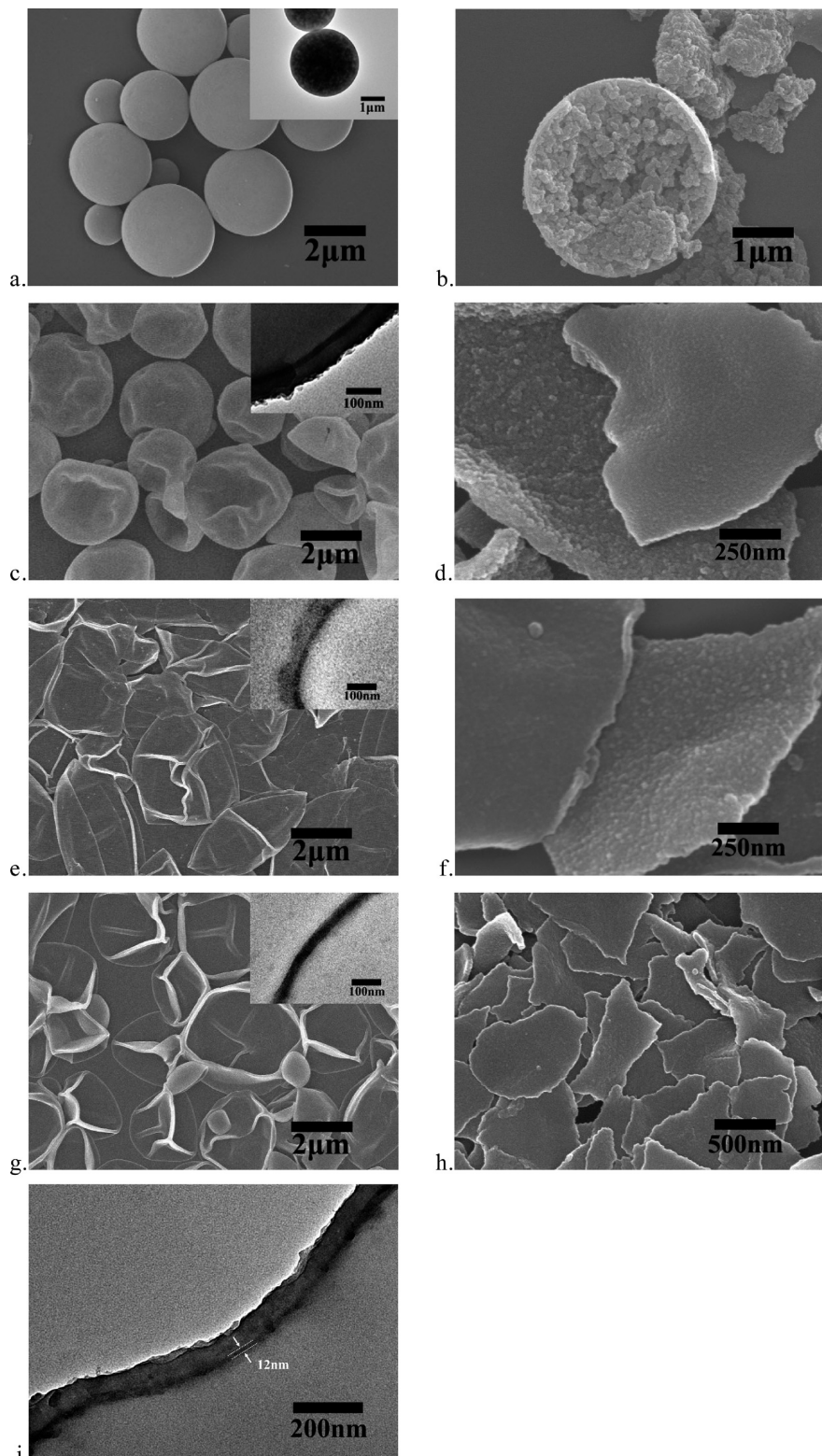


Figure 5. Some representative Janus polymer–inorganic composite hollow spheres and the corresponding Janus composite nanosheets synthesized at different DVB content (g): (a, b) 20; (c, d) 8; (e, f) 5; (g, h) 0. Silane content is fixed at 5.2 g. (i) Cross-section TEM image of the Janus hollow composite sphere at a low level of silane content (1.3 g).

Morphological evolution of the Janus hollow spheres with polymerization time was monitored (Figure 2). The interior shell surface is smooth before polymerization, meaning no polymer is grafted onto the surface of silica layer (Figure S1, Supporting Information). At an early stage of polymerization

(30 min), the grafted polymer layer is thin (Figure 2b). The spherical shape is not clear after drying (Figure 2a). With polymerization proceeding, the polymer layer becomes thicker and coarse. After 2–3 h polymerization, roughness and thickness of the shell changes less, meaning that polymerization is nearly

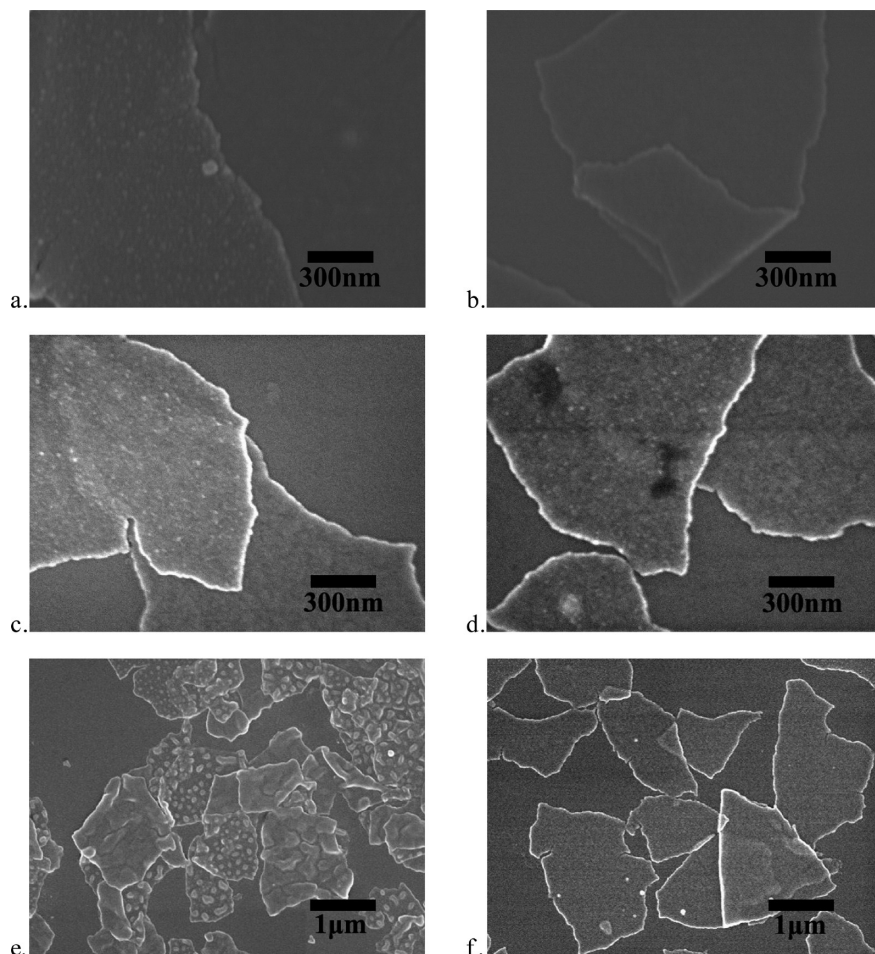


Figure 6. (a, b) SEM images of the Janus nanosheets with DVB as monomer in the absence of MPS before and after ultrasonication; (c–f) SEM images of the Janus nanosheets prepared with St as monomer: (c, d) with MPS before and after treatment with DMF; (e, f) without MPS before and after treatment with DMF.

completed (Figures 2c–f). This is consistent with kinetics of free radical polymerization. With polymerization time, the spherical contour becomes more distinct until the as-prepared hollow spheres (after 8 h polymerization) can well preserve their contour without collapse after drying (Figure 2, parts g and h). Strength enhancement of the hollow spheres is resulted from further sol–gel process of silica.^{9a}

Janus composite nanosheets were achieved by crushing the as-prepared Janus hollow spheres (Figures 3a). One side of the Janus nanosheets is rough corresponding to polymer, while the other one is smooth corresponding to silica. Trisodium citrate capped Au nanoparticles (about 15 nm in diameter) were used to selectively label the amine-terminated side by electrostatic interaction. The Au nanoparticles are preferentially conjugated onto the smooth side (Figure 3b), revealing that the smooth side contains amine- group.

At a given silica shell, polymer content of the Janus composite nanosheets is tunable with monomer DVB feeding amount in the oil phase. At a fixed silane amount, intensity of the characteristic bands assigned to PDVB increases with DVB feeding amount (Figure 4), meaning the increase of polymer content of the composite nanosheets. TGA results (Figure S5a, Supporting Information) further prove that the PDVB content increases with DVB feeding content (Figure S5b, Supporting Information). PDVB/silica weight ratio is tunable across 1:1. Besides PDVB content, microstructure of the Janus composite nanosheets is

controlled. At higher level of DVB (20 g) content, the interior surface of the Janus hollow spheres becomes much coarser until a polymer continuous porous network forms inside the cavity (Figure 5, parts a and b). At a low level of DVB content for example 8 g, the Janus hollow spheres partially collapse (Figure 5c). This can be explained by a weakening support of the polymer network to the shell. Cross section TEM image (inset Figure 5c) gives average thickness of the silica layer and PDVB layer about 20 and 57 nm, respectively. The PDVB surface of the Janus nanosheets becomes less coarse (Figure 5d). With further decrease of DVB content for example 5 g, the PDVB layer becomes thinner from 57 nm to about 47 nm (Figure 5e) with the silica layer thickness preserved. The PDVB side of the Janus nanosheets becomes nearly smooth (Figure 5f). In the absence of DVB, the Janus hollow spheres completely collapse (Figure 5g), and both sides of the Janus nanosheets are smooth (Figure 5h). Besides the polymer layer, thickness of the silica layer is tuned with silane content. For example, the silica layer becomes thinner to 12 nm at a low silane content level, for example, 1.3 g (Figure 5i).

MPS silane plays a key role in structural control of the Janus composite nanosheets. In the absence of MPS, although a rough side of the as-prepared Janus nanosheets is observed (Figure 6a), it becomes smooth after treatment by ultrasonication (Figure 6b). This is explained by removal of physically bound PDVB particles onto the surface. In contrast, in the

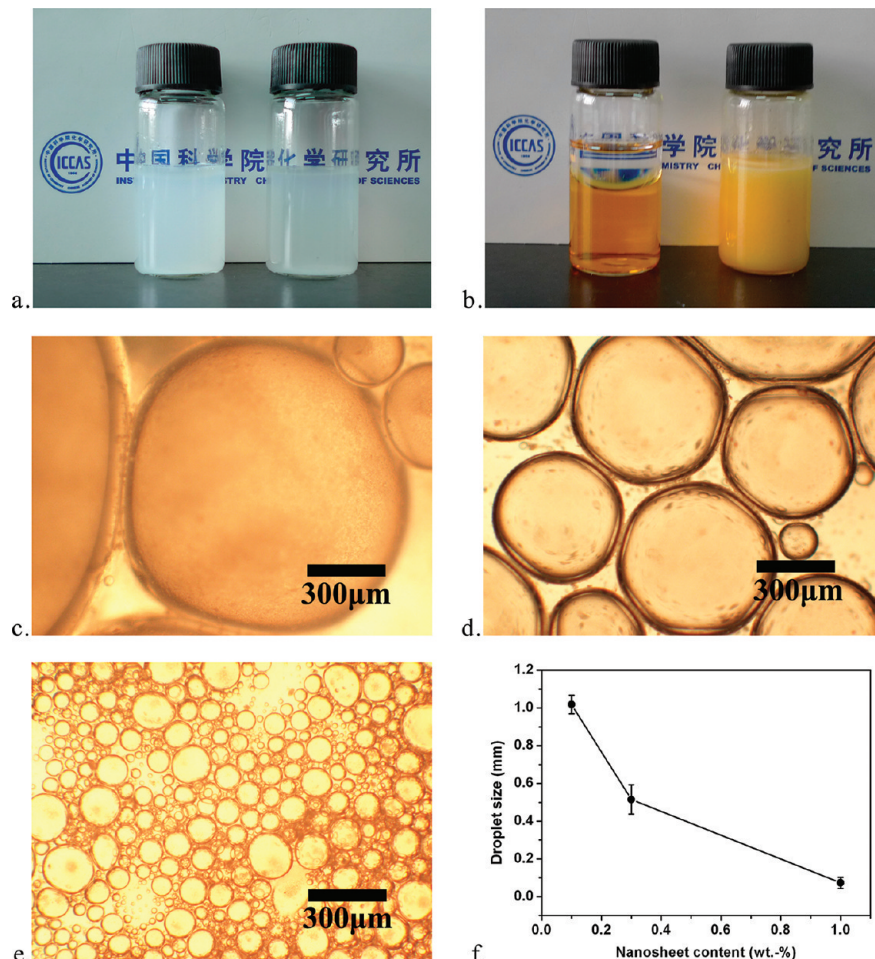


Figure 7. Emulsification of representative immiscible liquid mixture with the Janus composite nanosheets: (a) optical image of the Janus nanosheets dispersed in water (left) and toluene (right), respectively; (b) left: immiscible mixture of toluene (top) and water (bottom); right: water-in-toluene emulsion stabilized with the Janus nanosheet containing 69.6 wt % PDVB; water/toluene volume ratio is 2:1, and methyl orange is added to water as chromogenic agent; (c-e) optical microscopy image of the water-in-toluene emulsion stabilized with increasing Janus nanosheets: 0.1, 0.3, and 1.0 wt % respectively; (f) emulsion droplet diameter as a function of the Janus nanosheet content.

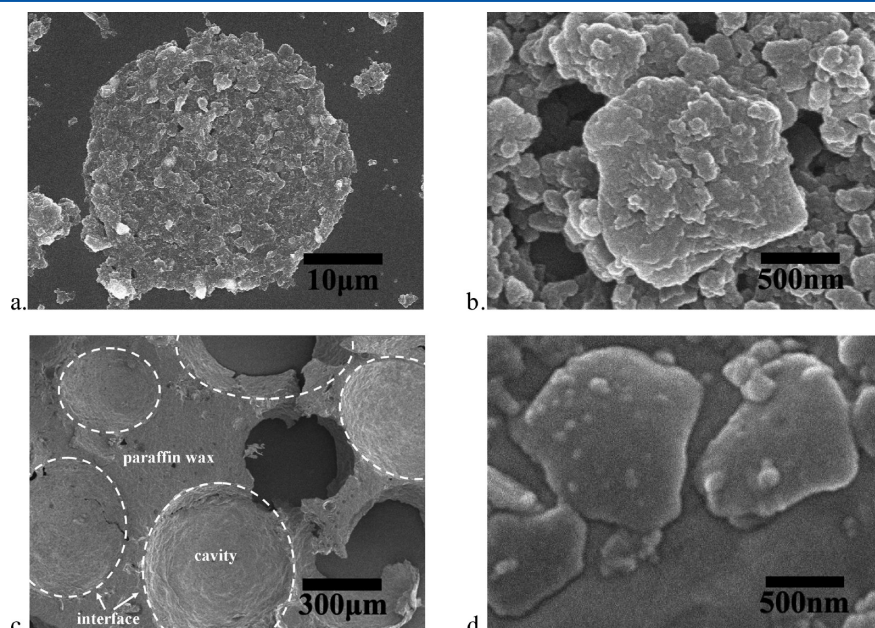


Figure 8. (a) SEM image of one emulsion drop of the water-in-toluene emulsion after drying and (b) the corresponding magnified image; (c) fracture SEM image of the cavity regions after water evaporates from the water-in-paraffin emulsion, orientation of the Janus nanosheets is frozen at the interface after paraffin is cooled to room temperature and (d) the corresponding magnified image.

presence of MPS, the rough surface remains, implying that PDVB is covalently bound. When styrene is used to replace DVB, the polymer side of the nanosheets remains rough, which is less influenced by treatment with DMF (Figures 6c, 6d). This means that a homogeneous PS brush has chemically grafted thereby. In comparison, in the absence of MPS, some lobes appear onto the interior surface (Figure 6e), which are easily dissolved with DMF (Figure 6f). This is explained by dewetting of PS onto silica surface. Since the side toward oil phase contains polymerizable vinyl group, the idea is universal to graft polymer brush onto the side by free radical polymerization. We have also tried to graft other polymer brushes, for instance poly(butyl acrylate) and poly(2-ethylhexyl acrylate).

The Janus composite nanosheets act as solid emulsifiers. As an example, the Janus nanosheets can be well dispersed both in water and toluene (Figure 7a), indicating that they are amphiphilic. Water and toluene are typically immiscible (Figure 7b). A trace of methyl orange was added into water phase for easy observation. In the presence of the Janus composite nanosheet containing 69.6 wt % of PDVB, a stable water-in-toluene (w/o) emulsion forms at a water/toluene volume ratio 2:1. The as-prepared emulsion keeps stable for several months. At 0.1 wt % of the nanosheet, the droplets are about 1 mm in diameter (Figure 7c). At 0.3 wt % of the nanosheet, the droplets become smaller ranging within 0.4–0.6 mm (Figure 7d). At a high level of nanosheet content for example 1.0 wt %, the droplets are about 0.1 mm (Figure 7e). The droplets become smaller with increase of Janus nanosheet content (Figure 7f).

The spherical contour is preserved after the emulsion drops are dried (Figure 8a). Magnified SEM image shows that the rough PDVB side faces the external oil phase (Figure 8b). In order to further observe orientation of the Janus nanosheet at the emulsion interface, a melt paraffin (T_m : 52–54 °C) was used instead of toluene. A water in melt-paraffin emulsion formed at 70 °C. After the paraffin was solidified upon cooling to room temperature, the Janus nanosheets were frozen at the interface. After dispersed water evaporated, some cavities were left (Figure 8c). Careful observation of the interior surface of the cavities shows that the smooth side of the Janus nanosheets faces internal water phase (Figure 8d). When water/oil volume ratio increases to higher level, for example, 9:1, continuous phase remains oil. This implies that the Janus composite nanosheets are more lipophilic. When the Janus composite nanosheet with lower PDVB content, for example, 22.1 wt %, was used, the continuous phase becomes water. In the case of lower water/toluene volume ratio, for example, 2:1, the continuous phase remains water. When water/toluene volume ratio is further decreased to 2:3, the continuous phase reverts to be oil. When the Janus silica nanosheet without PDVB was used, the continuous phase becomes water again at the water/toluene volume ratio 2:3. The fact indicates that Janus balance¹⁰ of the composite nanosheets is tunable across from more lipophilic to more hydrophilic. It is expected to finely tune microstructure of multiple component systems using such composite nanosheets with tunable Janus balance.

4. CONCLUSION

We have proposed a facile approach to large scale fabricate polymer–inorganic layered composite Janus nanosheets. The content and thickness of both polymer layer and inorganic layer are controllable. The Janus nanosheets can be used as solid surfactants to stabilize emulsions, whose Janus balance can be

greatly tunable crossing from more lipophilic to more hydrophilic. This method is general, and a huge family of polymer–inorganic composite Janus nanosheets with varied compositions and microstructures are derived.

■ ASSOCIATED CONTENT

S Supporting Information

TEM and SEM Janus silica hollow spheres images, particle size and distribution of one representative as-synthesized Janus hollow sphere, EDX spectra of the Janus hollow spheres, FT-IR spectra, and thermogravimetric analysis and PDVB/silica weight ratio. This material is available free of charge via the Internet at <http://pubs.acs.org/>.

■ AUTHOR INFORMATION

Corresponding Author

*E-mail: (F.L.) liangfuxin@iccas.ac.cn; (Y.C.) ylcai98@xtu.edu.cn; (Z.Y.) yangzz@iccas.ac.cn

■ ACKNOWLEDGMENTS

We thank Prof. Yunfeng Lu of UCLA for helpful discussion and careful reading of the manuscript to improve the writing. This work was supported by the NSF of China (50733004, 207201-02041, 51173191, and 50973121), MOST (2011CB933700, 2012CB933200), and CAS (KJCX2-YW-H20).

■ REFERENCES

- (1) de Gennes, P. G. *Rev. Mod. Phys.* **1992**, *64*, 645.
- (2) (a) Perro, A.; Reculusa, S.; Ravaine, S.; Bourgeat-Lami, E.; Duguet, E. *J. Mater. Chem.* **2005**, *15*, 3745. (b) Yang, S. M.; Kim, S. H.; Lim, J. M.; Yi, G. R. *J. Mater. Chem.* **2008**, *18*, 2177. (c) Walther, A.; Müller, A. H. E. *Soft Matter* **2008**, *4*, 663. (d) Wurm, F.; Kilbinger, A. F. M. *Angew. Chem., Int. Ed.* **2009**, *48*, 8412. (e) Wang, C.; Xu, C.; Zeng, H.; Sun, S. *Adv. Mater.* **2009**, *21*, 3045. (f) Jiang, S.; Chen, Q.; Tripathy, M.; Luijten, E.; Schweizer, K. S.; Granick, S. *Adv. Mater.* **2010**, *22*, 1060. (g) Trindade, A. C.; Canejo, J. P.; Pinto, L. F. V.; Patrício, P.; Brogueira, P.; Teixeira, P. I. C.; Godinho, M. H. *Macromolecules* **2011**, *44*, 2220. (h) Lattuada, M.; Hatton, T. A. *Nano Today* **2011**, *6*, 286.
- (3) (a) Binks, B. P.; Lumsdon, S. O. *Langmuir* **2001**, *17*, 4540. (b) Vignati, E.; Piazza, R. *Langmuir* **2003**, *19*, 6650.
- (4) (a) Binks, B. P.; Fletcher, P. D. I. *Langmuir* **2001**, *17*, 4708. (b) Glaser, N.; Adams, D. J.; Boker, A.; Krausch, G. *Langmuir* **2006**, *22*, 5227.
- (5) (a) Nonomura, Y.; Komura, S.; Tsujii, K. *Langmuir* **2004**, *20*, 11821. (b) Nonomura, Y.; Komura, S.; Tsujii, K. *J. Phys. Chem. B* **2006**, *110*, 13124.
- (6) (a) Walther, A.; André, X.; Drechsler, M.; Abetz, V.; Müller, A. H. E. *J. Am. Chem. Soc.* **2007**, *129*, 6187. (b) Walther, A.; Hoffmann, M.; Müller, A. H. E. *Angew. Chem., Int. Ed.* **2007**, *47*, 723.
- (7) (a) Dorvee, J. R.; Derfus, A. M.; Bhatia, S. N.; Sailor, M. J. *Nat. Mater.* **2004**, *3*, 896. (b) Bucaro, M. A.; Kolodner, P. R.; Taylor, J. A.; Sidorenko, A.; Aizenberg, J.; Krupenkin, T. N. *Langmuir* **2009**, *25*, 3876.
- (8) Gruning, B.; Holtschmidt, U.; Koerner, G.; Rossmy, G. US 4,715,986, 1987.
- (9) (a) Liang, F. X.; Liu, J. G.; Zhang, C. L.; Qu, X. Z.; Li, J. L.; Yang, Z. Z. *Chem. Commun.* **2011**, *47*, 1231. (b) Liang, F. X.; Shen, K.; Qu, X. Z.; Zhang, C. L.; Wang, Q.; Li, J. L.; Liu, J. G.; Yang, Z. Z. *Angew. Chem., Int. Ed.* **2011**, *50*, 2379.
- (10) Jiang, S.; Granick, S. *Langmuir* **2008**, *24*, 2438.
- (11) Jin, Z. G.; Wang, Y.; Liu, J. G.; Yang, Z. Z. *Polymer* **2008**, *49*, 2903.
- (12) Brinker, C. J.; Scherer, G. *Sol-Gel Science: The Physics and Chemistry of Sol-Gel Processing*; Academic Press: San Diego, CA, 1990; Chapter 3.
- (13) Frens, G. *Nat. Phys. Sci.* **1973**, *241*, 20.